

QUANTUM MECHANICAL PREDICTIONS OF ENERGETIC MATERIALS: WHEN GOOD THEORIES GO BAD

Edward F.C. Byrd,^{*} Cary F. Chabalowski and Betsy M. Rice
U. S. Army Research Laboratory
Aberdeen Proving Ground, MD 21005-5069

ABSTRACT

The performance of density functional theories (DFT) in predicting structural parameters for six conventional energetic materials (EM) over various degrees of compression was examined for a wide range of pressures. The systems studied were nitromethane, 1,3,5,7-tetranitro-1,3,5,7-tetraazacyclooctane (HMX), cyclotrimethylenetrinitramine (RDX), 2,4,6,8,10,12-hexanitrohexaazaisowurzitane (CL-20), 2,4,6-trinitro-1,3,5-benzenetriamine (TATB), and pentaerythritol tetranitrate (PETN). Dependencies of results on basis set size, k-points, choice of pseudopotential and method were explored. The results indicate that at zero compression, DFT is not adequate to describe crystallographic parameters for the systems under study. However, at compressions consistent with 6 GPa or greater, DFT predictions of crystal volumes are within 5% of experiment, and are insensitive to method, choice of pseudopotential and basis set size. The results suggest that the major source of error in DFT calculations applied to systems similar to these are due to inadequate treatment of van der Waals forces, which are the dominant forces in molecular organic crystals at the ambient state.

1. INTRODUCTION

Up to the last decade, available computing processing power limited theoretical treatment of condensed phase systems to classical molecular simulations methods such as molecular dynamics or Monte Carlo. While useful in predicting equation of state (EOS) information or providing temporal descriptors of the response of a material to stimuli, the accuracy of the results were almost completely dependent on the model used to describe the interatomic interactions. Additionally, such simulations cannot capture quantum effects such as tunneling, zero point energy, and electronic excitation. On the other hand, quantum mechanical methods do not suffer from these limitations, yet have been precluded from widespread use, particularly in condensed phase systems, due to their often inordinate computational requirements. In fact, even with the processing power available today, quantum mechanical treatments of condensed phase systems are largely restricted to the quantum mechanical method known as Density Functional Theory (DFT). DFT is routinely used to characterize large polyatomic molecules and certain condensed phase, materials (e.g.

metals, covalently bound systems). For those cases, DFT predictions demonstrate a high degree of accuracy. Unfortunately, DFT has also demonstrated some spectacular failures in predictive capabilities due to approximations in the implementation of the Density Functional Theory [Byrd et al., 2004]. Thus, evaluation of the suitability of this methodology when applied to material types for which extensive assessment has not been performed is required. Conventional CHNO energetic materials, which are organic molecular crystals, fall within this category of materials for which assessment of DFT applications is necessary. We present such an assessment through a review of our work which explores the suitability of various DFT methods applied to CHNO molecular crystals and their performance at different degrees of compression. [Byrd and Rice, 2007]

2. COMPUTATIONAL DETAILS

This work explores basis set, pseudopotential, method and k-point dependencies on predictions of crystal and molecular structural parameters for six well-studied conventional CHNO explosives under different degrees of compression. The systems are RDX, HMX, CL-20, nitromethane, PETN, and TATB. The GGA DFT Perdew-Burke-Ernzerhof (PBE) [Perdew et al., 1996] functional was also applied to nitromethane and RDX. All were subjected to the generalized gradient approximation density functional theory (GGA DFT) Perdew-Wang 91 (PW91) [Perdew, 1991] functional as implemented in the Vienna Ab-Initio Package (VASP) [Kresse and Furthermuller, 2003]. The Vanderbilt ultrasoft pseudopotentials (USP) [Vanderbilt, 1990] and Monkhorst-Pack k-point generation method were used for all calculations. Plane wave kinetic energy cut-offs (E_{cut}) ranged from 280 eV to 800 eV. Initial crystal structures used in the geometry optimizations correspond to experimental structures. In the geometry optimizations space group symmetry was not imposed and all ionic and cell degrees of freedom were allowed to vary. The electronic energies were converged to 2.0×10^{-6} eV, while the structures were converged once the difference in free energy between gradient steps was less than 2.0×10^{-5} eV. Smearing width was set to 0.0001 in the Methfessel-Paxton [Methfessel and Paxton, 1989] method minimized electron smearing, since molecular crystals are insulators. Also, the RMM-DIIS method was employed to accelerate

Report Documentation Page				Form Approved OMB No. 0704-0188	
Public reporting burden for the collection of information is estimated to average 1 hour per response, including the time for reviewing instructions, searching existing data sources, gathering and maintaining the data needed, and completing and reviewing the collection of information. Send comments regarding this burden estimate or any other aspect of this collection of information, including suggestions for reducing this burden, to Washington Headquarters Services, Directorate for Information Operations and Reports, 1215 Jefferson Davis Highway, Suite 1204, Arlington VA 22202-4302. Respondents should be aware that notwithstanding any other provision of law, no person shall be subject to a penalty for failing to comply with a collection of information if it does not display a currently valid OMB control number.					
1. REPORT DATE DEC 2008		2. REPORT TYPE N/A		3. DATES COVERED -	
4. TITLE AND SUBTITLE Quantum Mechanical Predictions Of Energetic Materials: When Good Theories Go Bad				5a. CONTRACT NUMBER	
				5b. GRANT NUMBER	
				5c. PROGRAM ELEMENT NUMBER	
6. AUTHOR(S)				5d. PROJECT NUMBER	
				5e. TASK NUMBER	
				5f. WORK UNIT NUMBER	
7. PERFORMING ORGANIZATION NAME(S) AND ADDRESS(ES) U. S. Army Research Laboratory Aberdeen Proving Ground, MD 21005-5069				8. PERFORMING ORGANIZATION REPORT NUMBER	
9. SPONSORING/MONITORING AGENCY NAME(S) AND ADDRESS(ES)				10. SPONSOR/MONITOR'S ACRONYM(S)	
				11. SPONSOR/MONITOR'S REPORT NUMBER(S)	
12. DISTRIBUTION/AVAILABILITY STATEMENT Approved for public release, distribution unlimited					
13. SUPPLEMENTARY NOTES See also ADM002187. Proceedings of the Army Science Conference (26th) Held in Orlando, Florida on 1-4 December 2008, The original document contains color images.					
14. ABSTRACT					
15. SUBJECT TERMS					
16. SECURITY CLASSIFICATION OF:			17. LIMITATION OF ABSTRACT UU	18. NUMBER OF PAGES 7	19a. NAME OF RESPONSIBLE PERSON
a. REPORT unclassified	b. ABSTRACT unclassified	c. THIS PAGE unclassified			

convergence except for those cases in which conjugate gradients were required to achieve convergence.

At zero pressure, basis set and k-point dependencies were explored for only four of the six systems (nitromethane, HMX, RDX and CL-20). At higher degrees of compression, planewave kinetic energy cut-offs (E_{cut}) were restricted to either 396 eV and/or 545 eV. Also at the higher degrees of compression, the Local Density Approximation (LDA) [Ceperley and Alder, 1980] functional was applied to TATB, PETN, and RDX. Because of concern over the adequacy of ultrasoft pseudopotentials for crystals under pressure, we used projected augmented wavefunction (PAW) [Blöchl, 1994; Kresse and Joubert, 1999] pseudopotentials to check for possible pseudopotential induced errors for the TATB and PETN crystals. To further eliminate pseudopotentials from consideration as the root of any error, norm-conserving Troullier-Martins pseudopotentials and the PBE functional as implemented in the PWSCF program package [Baroni et al., 2008] were used to predict crystal structures of compressed PETN. For these calculations, optimized geometries were obtained using a damped molecular dynamics calculations, with convergence criteria for electron energies set at 1.0×10^{-9} Rydberg and total energy convergence set at 1.0×10^{-6} Rydberg. The final converged geometries were obtained through a damped molecular dynamics calculation as coded in PWSCF. k-point meshes employed for non-zero pressures were: $2 \times 1 \times 2$ for HMX, $1 \times 1 \times 1$ for RDX and CL-20, $2 \times 2 \times 2$ for TATB, and $2 \times 2 \times 2$ for PETN. The Troullier-Martins PBE PWSCF calculations used only the gamma point. Initial structures used in the geometry optimizations of all crystals under all degrees of compression correspond to the ambient pressure experimental crystal structure.

3. RESULTS AND DISCUSSION

3.1 Predictions for crystals with no compression

Starting with investigating the zero compression crystals, for each of the four crystals for which basis set and k-point dependencies were explored (nitromethane [Trevino et al., 1980], HMX [Choi and Boutin, 1970], RDX [Choi and Prince, 1972], CL-20 [Nielsen et al., 1998]), the grid that had the minimum number of k-points that gave a converged result was identified. Once the grid was identified, crystallographic and molecular structural parameters were calculated for kinetic energy cutoffs ranging between 280 and 800 eV. The resulting grids for nitromethane and HMX are $(2 \times 2 \times 2)$ and $(2 \times 1 \times 2)$, respectively. For RDX and CL-20, we determined the $(1 \times 1 \times 1)$ was sufficient to yield converged results.

Predicted molecular structural parameters (bond lengths and bond angles) were converged between 495 and 545 eV, and once converged, are in excellent agreement with measured values. Mean errors in bond lengths for all four systems are no more than 0.017 Å, with the mean error in bond lengths for CL-20 an order of magnitude smaller. The maximum errors using a sufficient basis set for bond distances is less than 0.04 Å for nitromethane, RDX and HMX, and 0.02 Å for CL-20. Similar to predictions for isolated molecules, the DFT predictions of molecular structural parameters are in very good agreement with experimental values. However, for the crystallographic structural parameters, we observe poor convergence to erroneous values. This is illustrated in Figure 1, which shows the percent error in lattice parameters as a function of kinetic energy cutoff for nitromethane, HMX, RDX and CL-20.

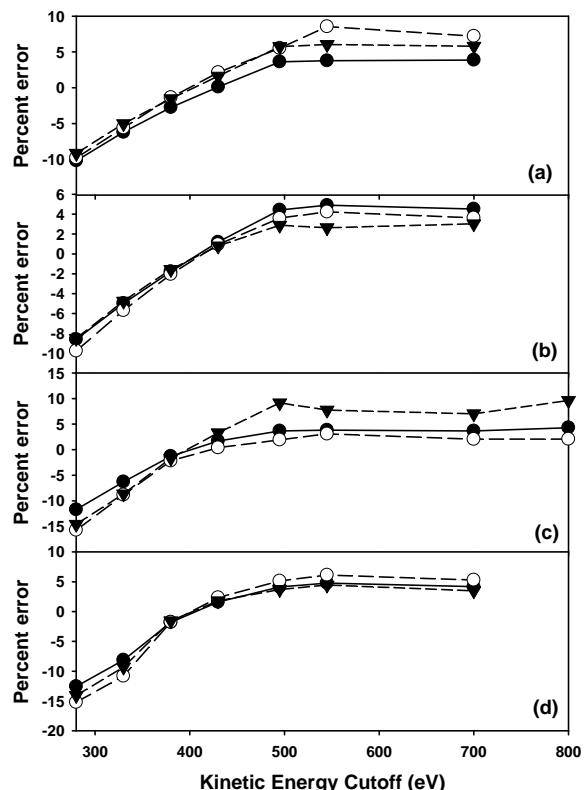


Figure 1. Variation of lattice dimensions with pressure for (a) nitromethane, (b) HMX, (c) RDX, and (d) CL-20. The a , b , c -cell constants are represented by circles, open circles and triangles, respectively.

The range of kinetic energy cutoffs for three of the systems is 280 to 700 eV; an additional point was calculated for RDX at 800 eV since it was not clear that the results had converged at 700 eV. It is interesting to note that at around 400 eV, near the default cutoff value in VASP for an oxygen containing compound (395 eV), the percent error in lattice parameters for all systems is approximately zero. However, the results do not begin to converge until 545 eV, but do so to values between 5 to

10% too large. Although not shown in these figures, we observe similar behavior for TATB and PETN. We should point out that space group symmetry is conserved in the geometry optimization, and for the two non-orthorhombic cells (CL-20 and HMX), the deviation of the non-90° angle is within 1.5° of experiment.

These errors in the lattice vectors could be inherent to the PW91 functional. To explore this possibility, we calculated crystallographic parameters using the PBE functional as implemented in the VASP suite using E_{cut} of 495, 545, and 645 eV for nitromethane and E_{cut} of 430 and 495 eV for RDX. Figure 2 illustrates the errors in the a , b , and c lattice vectors for both nitromethane and RDX with this method; results using the PW91 functional are provided for comparison. As evident in the figure, although the results using the PBE functional are smaller than those generated using the PW91 functional, the improvement is not substantial enough to conclude that the major source of error is in the choice of the PW91 functional. More likely, the major source of error is due to the inherent deficiencies in DFT to appropriately model van der Waals forces, which are the main binding forces in molecular organic crystals such as these.

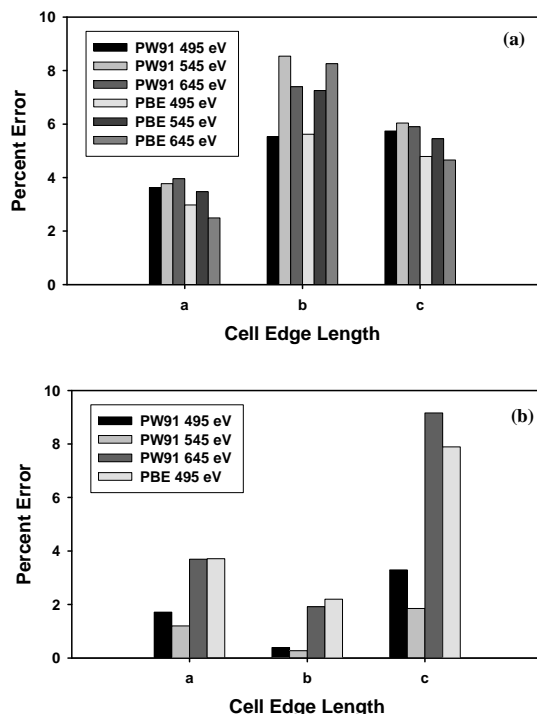


Figure 2. Comparison of percent errors versus experiment for cell lengths between PW91 and PBE for (a) nitromethane and (b) RDX

3.2 Predictions at varying degrees of compression

Although DFT is clearly unable to adequately predict crystal structures of energetic molecular crystals at zero

compression, there are studies indicating weakly-bound molecular systems under sufficient compression can be reasonably described by DFT [Miao et al., 2003]. This, as well as our interests in theoretical characterization of energetic materials under extreme conditions (including high compression), we explored the ability of conventional DFT to predict structures of energetic materials under high compression. Also, we were interested in determining the degree of compression for which DFT could suitably treat the EM; i.e. those pressure regimes for which dispersion is not the dominant component of the interactions. Therefore, we calculated crystallographic and intramolecular parameters for five energetic molecular crystals under varying degrees of compression. In this paper, we report results only for the systems for which there are extensive experimental information over a large pressure range (TATB [Olinger and Cady, 1974], HMX [Olinger et al., 1978], and PETN [Olinger et al., 1975]). We have also calculated structural parameters of compressed RDX [Olinger et al., 1978] and CL-20 [Sorescu et al., 1998]; however, both systems undergo polymorphic phase changes at relatively low pressures, and therefore, there are limited experimental data available for comparison.

As in the study described in Section 3.1, we explored dependencies of the results on basis set size, choice of pseudopotential, and specific implementations of DFT. With regard to the latter point, we performed calculations using the 545 eV planewave basis set and Vanderbilt ultrasoft pseudopotentials (USP) using LDA and GGA (PW91 and PBE) methods. LDA volumes for the TATB and PETN crystals at zero pressures are smaller than experiment by 11% and 15%, respectively. As pressures increase, LDA errors for TATB and PETN decrease to 4% too small at 7 GPa for TATB and 7% too small at 10 GPa for PETN. Unlike the LDA results, the GGA methods predict lattice parameters that are substantially larger than the experimental values at zero pressure, with deviations of the predictions from experiment decreasing with increasing pressure. This behavior is apparent in Fig. 3, which shows the behavior of the volume and lattice parameters of PETN with increase in pressure for the various methods. For all calculations at all pressures, the space group symmetry was maintained in the completely unconstrained geometry optimizations.

Extensive structural analyses of the contents of the unit cells for all crystals subjected to compression were to determine any pressure-dependent rotational and translational disorder of the molecules within the unit cell. Because detailed experimental data about atomic positions in the crystals are lacking for pressures above 1 atm., we are limited to structural comparisons with experimental crystal structures at room conditions. Unit cell degrees of freedom that will be compared are the six cell constants (a , b , c , α , β , γ) and the orientational and

translational degrees of freedom of each of the molecules in the unit cells. The molecular translational degrees of freedom will be given in fractional coordinates (s_x , s_y , s_z) of the molecular mass centers. Euler angles for rigid-body rotation about inertial axes (θ , ϕ , ψ) for all molecules in the unit cell are used to describe the molecular orientational degrees of freedom. Symmetry constraints were not imposed in the geometry optimizations, therefore, the molecules within the unit cell are not required to be symmetry equivalents. Thus, molecular translational and orientational parameters for each molecule within the unit cell were examined.

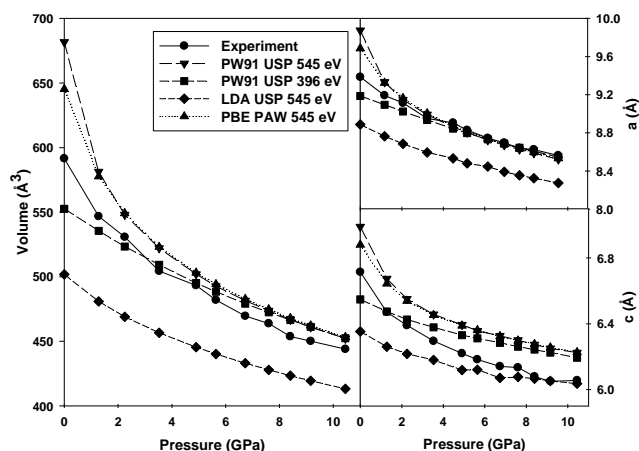


Figure 3. Variation of volume and lattice dimensions with pressure for PETN.

For RDX, fractional coordinates of the molecular mass centers differ slightly from those in the ambient-state crystal, with differences in the thousandths. Orientation of the molecules about any one of the Euler angles is no greater than 3° , resulting in a root-mean square (rms) deviation of the predicted atomic displacements from the experimental positions of 0.064 \AA and a maximum atomic displacement is 0.229 \AA . Molecular structural parameters for ϵ -CL-20 generated at 2.5 GPa are in similar close agreement with the ambient state crystal.

The differences in fractional coordinates of the molecular mass centers for β -HMX and TATB are similar to those of RDX up to 4 GPa, but deviations of the fractional coordinates become as large as 0.011 at higher degrees of compression. Deviations in the Euler angles are no greater than 2° over the pressure ranges. For TATB, the rms deviations in atomic displacements are all $\sim 0.1 \text{ \AA}$, and are attributed to the difference in the orientation of the amine groups relative to the ring. In experiment, the amine hydrogens are out of the plane of the molecule, whereas in the theoretical calculations, all atoms lie in approximately within a plane.

Four of the five systems studied are relatively rigid molecules, three of which are cyclic nitramines and one a nitroaromatic. The remaining molecule, PETN, however, is an acyclic, branched-chain molecule that would more readily deform upon compression. This expectation is supported by results from diamond anvil cell (DAC) experiments indicating a conformation change to a lower-symmetry molecular structure after subjecting the system to pressures greater than 5 GPa [Grudzkov et al., 2004]. A second group performed a series of DAC experiments in which changes in PETN with high pressure were monitored [Lipinska-Kalita et al., 2005]. These experiments were performed without and with a pressure-transmitting medium (nitrogen), with the latter designed to provide quasi-hydrostatic conditions. A structural phase transition was apparent at 8 GPa in the experiments in which the pressure-transmitting medium was not present, but results in which nitrogen was introduced into the cell indicated that any structural rearrangements due to compression under these experimental conditions are fully reversible. These authors conclude that the discrepancies between the two sets of measurements are due to differences in the experimental condition specifically that more severe non-hydrostatic conditions are introduced in the absence of the pressure-transmitting medium. Our calculations represent pure hydrostatic compression; differences in fractional coordinates are less than 0.03 over the entire range of pressures studied, with differences in the Euler angles are no greater than 3.5° . At the largest pressure (10.45 GPa), the rms deviation of the atomic displacement is 0.117 \AA and the maximum deviation is 0.170 \AA . A graphical depiction of the predicted unit cell at 10.45 GPa superimposed on the experimental cell at ambient conditions is given in Fig. 4, demonstrating the small deformation of the molecular structure at high degrees of compression. The results presented here are supportive of the suggestion that under quasi-hydrostatic compression, no irreversible structural changes occur. However, additional experimentation or theoretical investigation of non-hydrostatic compression needs to be performed to provide a definitive conclusion.

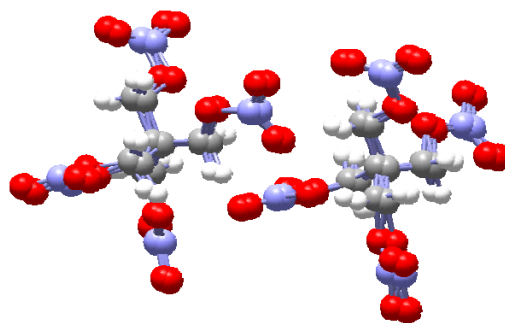


Figure 4. Pictorial view of the 10.45 GPa PW91 (545 eV) unit cell structure of PETN superimposed onto the ambient pressure experimental unit cell.

Basis set size dependencies for compressed crystals were also investigated using the PW91 functional and 396 eV kinetic energy cutoff. For pressures greater than 6 GPa, the predictions using the 396 eV and 545 eV basis sets converge to the same values, and are all slightly larger than experiment. However, the error is substantially less than that at 545 eV and zero pressure. A larger kinetic energy cutoff (645 eV) was utilized in calculations for two pressures for each of TATB and PETN to ensure that the 545 eV kinetic energy cutoff produced converged results; the difference between the predicted volumes at the various pressures were less than 2 \AA^3 for all cases.

The results also appeared to be insensitive to choice of functional. For pressures greater than 2 GPa, PBE using PAW pseudopotentials and PW91 using USP converge to the same result, again illustrated for PETN in Figure 3. Finally, to ensure that the softer PAW and ultrasoft pseudopotentials were not contributing to error at compression, we employed an extremely hard Troullier-Martins (TM) pseudopotential with a series of planewave basis sets for PETN. The results indicate that the converged TM results (using extremely large basis sets) are comparable to those generated using the softer pseudopotentials. As an added bonus, these calculations, which were performed using the software suite PWSCF [Baroni et al., 2008], have allowed us to eliminate as possible sources of error the specific implementations of quantum mechanical methods in different software packages.

4. FUTURE DIRECTIONS

We are in the process of evaluating emerging methods designed to remedy the deficiency of conventional DFT, *i.e.* its improper treatment of dispersion. To date, we have explored a method developed by Langreth (vdW-DFT) [Rydberg et al., 2003; Dion et al., 2004] to correct for the inadequate treatment of van der Waals in DFT [Hooper et al., 2008]; however, while yielding improved results over conventional DFT, the approach was computational unwieldy. We also exploring other alternatives, including new functionals developed by University of Minnesota (the M0X series) [Zhao et al., 2005; Zhao et al., 2006; Zhao and Truhlar, 2008a, 2008b] and Dispersion Corrected Atom Centered Pseudopotentials (DCACPs) [von Lilienfeld et al., 2004; von Lilienfeld et al., 2005; Tkatchenko and von Lilienfeld, 2006; von Lilienfeld and Andrienko, 2006].

Initially, the M0X functions were not employed in any periodic DFT codes, but only in molecular codes; thus, we assessed the functionals for various dimers while concurrently augmenting CP2K (see discussion on CP2K above) to accommodate the M0X family of functionals.

While efforts are ongoing to implement M0X functionals into CP2K, initial results for this family of functionals [Hooper, 2008] suggest these functions are promising. Figure 5 shows the binding energy of an RDX dimer using the M05 functional, the Langreth method (vdW-DFT), conventional PBE DFT and the highly accurate (and extremely computationally expensive) SAPT method. Not surprisingly, the standard PBE DFT performs poorly when compared to SAPT, while the other DFT methods are more accurate. While the vdW-DFT is in closer agreement with the SAPT value, one must take into account that this method requires 30-50% more calculation time per point than the M05 method. As the more advanced M06 models are coded, we expect to see an improvement over the results predicted with M05.

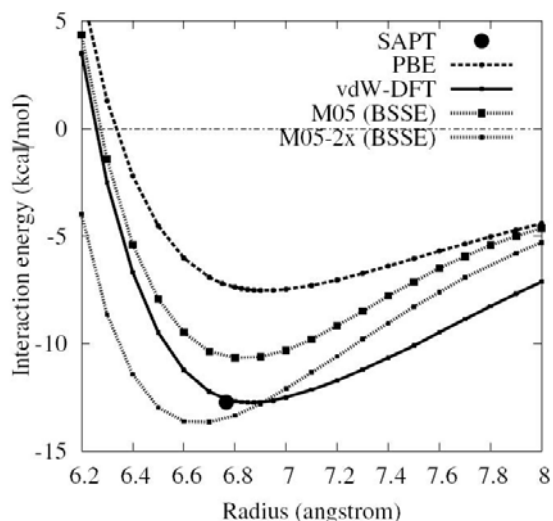


Figure 5. Binding Energy as a function of RDX dimer separation [Hooper, 2008].

We are in the process of investigating the accuracy of DFT calculations of molecular crystals using DCACPs, a capability developed to include van der Waals interactions in a self-consistent manner within the framework of DFT. This capability was present in CP2K, and we have begun an exploration into its performance when applied to HMX, RDX, TATB and PETN at zero compression (where conventional DFT fails) as well as at the higher-pressure regimes where conventional DFT better performs. The results will be compared both with experimental information and with calculations using conventional DFT.

Calculations to date have only explored the dependence of the results on basis set size. All calculations were performed using TZVP basis sets and the PBE functional using DCACPs. We intend to perform a series of calculations for those systems for which conventional DFT fails, *i.e.* HMX, PETN, TATB and RDX. Preliminary results for PETN are shown in Fig. 6.

Additionally calculations for the same system using conventional DFT and the PBE functional are given for comparison. It is clear that for PETN, the PBE functional using DCACPs performs quite well in predicting the low pressure crystal structure.

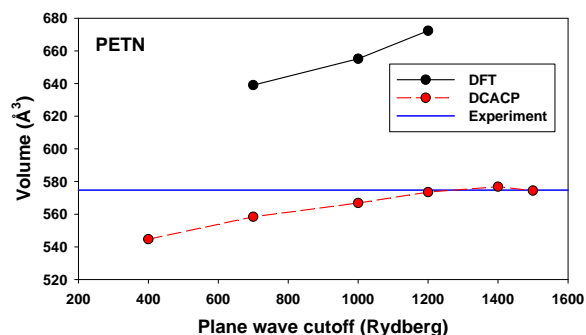


Figure 6. Unit Cell volumes versus plane wave cutoff for PETN. Black circles and lines denote conventional DFT results; red circles and lines denote DCACP DFT results

CONCLUSIONS

We have presented a review of our efforts to evaluate the performance of various density functional theories when applied to a few common energetic materials both at zero pressure and under compression. The results show that DFT is not suitable for accurate prediction of crystallographic parameters of these systems at low degrees of compression; percent differences from experimental volumes range from 10 to 16% for the systems studied. However, molecular structural parameters at zero pressure are in good agreement with experimental values. At higher pressures, PW91 and PBE functionals converged to the same results regardless of basis set or pseudopotential and over-predict experimental volumes by approximately 5%.

These results support the hypothesis that the majority of the error in these calculation at low compression due to inadequate treatment of the weak binding forces in molecular crystal (i.e. van der Waals forces). However, the results clearly indicate that for compression regimes in which other intermolecular forces dominate, DFT is a suitable method to predict crystallographic parameters.

ACKNOWLEDGEMENTS

This work was supported by the US Army Research, Development and Engineering Command Environmental Quality Technology Ordnance Program and the Office of Naval Research. All calculations were performed at the DoD Major Shared Resource Centers

located at the Army Research Laboratory and the Air Force Research Laboratory.

REFERENCES

- Baroni, S., Dal Corso, A., de Gironcoli, S., Giannozzi, P., <http://www.pwscf.org>.
- Blöchl, P.E., 1994, Projector augmented-wave method, *Phys. Rev. B*, **50**, 17953.
- Byrd, E.F.C., Scuseria, G.E., Chabalowski, C.F., 2004: An ab Initio Study of Solid Nitromethane, HMX, RDX, and CL20: Successes and Failures of DFT, *J. Phys. Chem. B* **108**, 13100.
- Byrd, E.F.C., Rice, B.M., 2007: Ab Initio Study of Compressed 1,3,5,7-Tetranitro-1,3,5,7-tetraaza-cyclooctane (HMX), Cyclotrimethylenetrinitramine (RDX), 2,4,6,8,10,12-Hexanitrohexaazaisowurzitane (CL-20), 2,4,6-Trinitro-1,3,5-benzenetriamine (TATB), and Pentaerythritol Tetranitrate (PETN), *J. Phys. Chem. C* **111**, 2787.
- Ceperley, D.M., Alder, B.J. 1980: Ground state of the electron gas by a stochastic method, *Phys. Rev. Lett.* **45**, 566.
- Choi, C.S., 1972: Crystal structure of cyclotrimethylenetrinitramine, *Acta Crystallogr. B* **28**, 2857.
- Choi C.S., Boutin H.P., 1970: Study of the crystal structure of β -cyclotetramethylenetetranitramine by neutron diffraction, *Acta Crystallogr Sect B* **26**, 123.
- Dion, M., Rydberg, H., Schroder, E., Langreth, D.C., Lundqvist, B.I., 2004: Van der Waals density functional for general geometries, *Phys. Rev Lett.* **92**, 246401.
- Gruzdkov, Y.A., Dreger, Z. A. and Gupta, Y. M.. 2004: Experimental and Theoretical Study of Pentaerythritol Tetranitrate Conformers, *J. Phys. Chem. A* **108** 6216.
- Hooper, J., 2008: private communication.
- Hooper, J., Cooper, V., Thonhauser, T., Romero, N., Zerilli, F., and Langreth, D.C. (2008): Predicting C-H/ π interactions with nonlocal density functional theory, *Chem. Phys. Chem.* **9**, 1216.
- Kresse, G., Furthmüller J., 2003: *Vienna Ab-initio Simulation Package (VASP): The Guide*, VASP Group, Institut für Materialphysik, Universität Wien: Sensengasse 8, A-1130 Wien, Vienna, Austria.
- Kresse, G., Joubert, D., 1999: From ultrasoft pseudopotentials to the projector augmented-wave method, *Phys. Rev. B*, **59**, 1758.
- Lipinska-Kalita, K. E., Pravica, M.G. and Nicol, M., 2005: Raman Scattering Studies of the High-Pressure Stability of Pentaerythritol Tetranitrate, *C(CH₂ONO₂)₄*, *J. Phys. Chem. B* **109**, 19233.
- Methfessel, M., Paxton, A.T., 1989: High-precision sampling for Brillouin-zone integration in metals *Phys Rev B* **40**, 3616.

- Miao M.S., Doren V.E., Martins J.L., 2003: Density-functional studies of high-pressure properties and molecular dissociations of halogen molecular crystals, *Phys Rev B* **68**, 094106.
- Nielsen A.T., Chafin A.P., Christian S.L., Moore D.W., Nadler M.P., Nissan R.A., Vanderah D.J., Gilardi R.D., 1998: George C.F., Flippen-Anderson, J.L. Synthesis of polyazapolycyclic caged polynitramines, *Tetrahedron* **54**, 11793.
- Olinger, B.W., Cady, H.H., 1976: Hydrostatic compression of explosives and detonation products to 10 GPa (100 kbars) and their calculated shock compression : results for PETN, TATB, CO₂ and H₂O, *Sixth Symposium(International) on Detonation*, 700.
- Olinger, B.W., Halleck, P.M., Cady, H.H., 1975: The isothermal linear and volume compression of pentaerythritol tetranitrate (PETN) to 10 GPa (100 kbar) and the calculated shock compression, *J. Chem. Phys.* **62**, 4480.
- Olinger, B.W., Roof, B., Cady, H.H., 1978 : The linear and volume compression of β -HMX and RDX to 9 GPa (90 kilobar). *Symposium international Sur Le Comportement Des Milieus Denses Sous Hautes Pressions Dynamiques*, Commissariat a l'Energie Atomique Centre d'Etudes de Vajours: Paris, France, 3.
- Perdew, J.P., 1991: in *Electronic Structures of Solids '91*, Ziesche, P. Eschrig, H., Eds., Akademie-Verlag: Berlin.
- Perdew, J.P., Berke, K., Ernzerhof, M., 1996: Generalized Gradient Approximation Made Simple, *Phys. Rev. Lett.* **77**, 3865.
- Rydberg, H., Dion, M., Jacobson, N., Schroder, E., Hyldgaard, P., Simak, S., Langreth, D.C., Lundqvist, B.I., 2003: *Phys. Rev. Lett.* **91**, 126402.
- Sorescu, D. C., Rice, B.M., and Thompson, D.L., 1998: Molecular Packing and NPT-Molecular Dynamics Investigation of the Transferability of the RDX Intermolecular Potential to 2,4,6,8,10,12-Hexanitrohexaazaisowurtzitane *J. Phys. Chem. B* **102**, 948.
- Tkatchenko, A., von Lilienfeld, O. A., 2006: Adsorption of Ar on graphite using London dispersion forces corrected Kohn-Sham density functional theory, *Phys. Rev. B* **73**, 153406.
- Trevino S.F., Prince E., Hubbard C.R., 1980: Refinement of the structure of solid nitromethane, *J. Chem. Phys.* **73**, 2996.
- Vanderbilt, D. 1990: Soft self-consistent pseudopotentials in a generalized eigenvalue formalism, *Phys Rev B.* **41**, 7892.
- von Lilienfeld, O. A., Andrienko, D., 2006: Coarse-grained interaction potentials for polyaromatic hydrocarbons, *J. Chem. Phys.* **124**, 054307
- von Lilienfeld, O. A., Tavernelli, I., Rothlisberger, U., Sebastiani, D., 2004: Optimization of effective atom centered potentials for London dispersion forces in density functional theory, *Phys. Rev. Lett.* **93**, 153004.
- von Lilienfeld, O. A., Tavernelli, I., Rothlisberger, U., Sebastiani, D., 2005: Performance of optimized atom-centered potentials for weakly bonded systems using density functional theory, *Phys. Rev. B* **71**, 195119.
- Zhao, Y. and Truhlar, D. G., 2008a: The M06 suite of density functionals for main group thermochemistry, thermochemical kinetics, noncovalent interactions, excited states, and transition elements: two new functionals and systematic testing of four M06-class functionals and 12 other functionals, *Theor. Chem. Acc.* **120**, 215.
- Zhao, Y. and Truhlar, D. G., 2008b: Density Functionals with Broad Applicability in Chemistry, *Acc. Chem. Res.* **41**, 157.
- Zhao, Y., Schultz, N. E., Truhlar, D. G., 2005: Exchange-correlation functional with broad accuracy for metallic and nonmetallic compounds, kinetics, and noncovalent interactions, *J. Chem. Phys.* **123**, 161103.
- Zhao, Y., Schultz, N. E., and Truhlar, D. G., 2006: Design of Density Functionals by Combining the Method of Constraint Satisfaction with Parametrization for Thermochemistry, Thermochemical Kinetics, and Noncovalent Interactions, *J. Chem. Theory Comput.* **2**, 364.